Relaxation of candidate electron spin qubits

S.A. Lyon
Department of Electrical Engineering, Princeton University, Princeton, NJ 08544

ABSTRACT

We have recently measured pulsed electron spin resonance (ESR) from electrons bound to donors in silicon. Measurements made in the late 1950's showed that these spins were long-lived, but we find coherence times that are about two orders of magnitude longer than previously seen. We have also measured the spin-decoherence of free, 2-dimensional electrons in an ultra-high mobility Si/SiGe quantum well. The coherence time of the 2D electron spins is long in comparison to compound semiconductor systems, but several orders of magnitude shorter than that of the donor-bound electrons. Spin-orbit coupling in the form of the Structural Inversion Asymmetry (Rashba effect) appears to be the cause of the increased decoherence rate of the 2D electrons' spin. For architectures employing quantum dots at a heterointerface, the Rashba effect is not expected to cause a loss of spin coherence while the electron is in the ground state, but thermal excitation to upper dot levels could lead to decoherence. We discuss ways in which this Rashba term can be minimized in Si-based structures, as well as other physical systems (electrons on liquid helium, for example) in which much longer spin coherence times can be expected.

Keywords: qubit, spin relaxation, quantum information, electron spin resonance, Si, electrons on liquid helium, decoherence

Electron spins are prime candidate for qubits in a several quantum information processing proposals.[1,2,3,4] There are a number of reasons for the popularity of electron spins. First is the fact that the spin of an electron is a well-studied, well-understood two-level system.[5] In part, the fact that electron spins have been studied so extensively is due to their long coherence times. This in turn arises from the weakness of the magnetic interactions that govern the evolution of the spins. Weak interactions allow for long time-scale measurements. While other two-level systems (certain electronic excitations[6], for example) may remain coherent for as large or a larger number of cycles, the readily accessible transition frequencies and long absolute coherence times of spins make experiments on them relatively straightforward.

A second major reason for using electron spins is that the electrons can be easily moved and manipulated. Nuclei often have even much longer spin coherence times than electrons, but it is generally much more difficult to manipulate them. In particular, a huge industry has built up around the control of electron motion in semiconductors. This technological base is one of the key advantages of electron spins as candidate qubits.

It has been known for close to half a century that electron spins in semiconductors, particularly Si, can have very long relaxation times, both longitudinal (T_1) and transverse (T_2, which for isolated spins can be associated with the spin coherence time). Silicon is a particularly good choice among semiconductors for low-decoherence electron spins. First, it is lightest element among the common semiconductors, which leads to a relatively low spin-orbit interaction. Being an elemental semiconductor with a cubic crystal structure, inversion symmetry further limits the strength of the coupling.[7] Beyond that, the position of the conduction band minima in Si near the X-point in the Brillouin zone reduces the spin-orbit effects even more.[8] Thus, as compared to other common semiconductors, the interactions of a spin with the host material for electrons in Si is particularly weak.

Another intrinsic advantage of Si is the relatively small natural abundance of isotopes with a nonzero nuclear spin. The only stable such isotope is ^{29}Si, and it constitutes only 4.68% of natural silicon. Isotopically purified Si is also readily available. Magnetic nuclei can couple to the electron spins, both through the hyperfine interaction and through the direct magnetic dipole-dipole interaction. The interaction with the ^{29}Si leads to a broadening of the Electron Paramagnetic Resonance (EPR) lines of electrons in Si. A particular case we will consider below is that of an electron bound to a shallow impurity (donor) where the broadening of the EPR signal in natural Si is about 0.1% (or about 3 Gauss in a 3500 Gauss field).

Noise and Information in Nanoelectronics, Sensors, and Standards II, edited by Janusz M. Smulko, Yaroslav Blanter, Mark I. Dykman, Laszlo B. Kish, Proc. of SPIE Vol. 5472 (SPIE, Bellingham, WA, 2004) · 0277-786X/04/$15 · doi: 10.1117/12.550634

Combining the advantages of electron spins with those of using Si as a host material, and it is clear why electrons in Si are promising qubit candidates. We will discuss recent experiments on the spin coherence times which can be obtained in Si. We find very long coherence times for the spin of electrons bound to phosphorus donors in Si,[9] but considerably shorter times for free 2D electrons at Si/SiGe interfaces.[10] The shorter times for the 2D electron gas (2DEG) can be explained as a consequence of spin-orbit coupling, and shows that tight confinement of electrons (as in the donors) is needed to obtain very long coherence times. Unfortunately, keeping the electrons tightly confined on a donor or in a quantum dot partially defeats one of the purposes of using electron spins as a qubit – the ability to move the electron easily through the semiconductor. However, if the electrons are held at the surface of liquid helium, instead of at a semiconductor heterointerface, the atomic contribution to the spin-orbit interaction is eliminated and electrons can be moved without significant decoherence.

The samples used for the 2D electron experiments were grown by MBE, with a 0.5 μm strain-relaxed $Si_{0.75}Ge_{0.25}$ buffer atop a 2-2.5 μm compositionally graded $Si_{1-x}Ge_x$ layer, followed by the Si quantum well, doped $Si_{0.75}Ge_{0.25}$ layers and a Si cap. The details of the growth and electrical measurements have been described elsewhere.[11] The experiments reported here were performed on structures with a 20nm quantum well. The modulation doping density was kept low in these samples and little or no EPR signal is observed initially. However, electrons can be introduced into the quantum well by illumination and persistent photoconductivity.[12] After sufficient illumination there is a Fermi-degenerate electron system with a density of $3x10^{11}/cm^2$ and a mobility of about $9x10^4$ $cm^2/V\text{-}s$.[13]

The measurements were performed with a Bruker Elexsys580 X-band EPR spectrometer using a dielectrically loaded cylindrical resonator (EN-4118MD4). The sample was held in a fused silica tube, immobilized with frozen ethanol, and the entire cavity and sample maintained at low temperature (4-5K) with a helium-flow cryostat (Oxford CF935). The temperature was controlled to better than 0.05K with a calibrated Cernox temperature sensor, though no temperature dependence was found over the range from 3.5 to 8K.

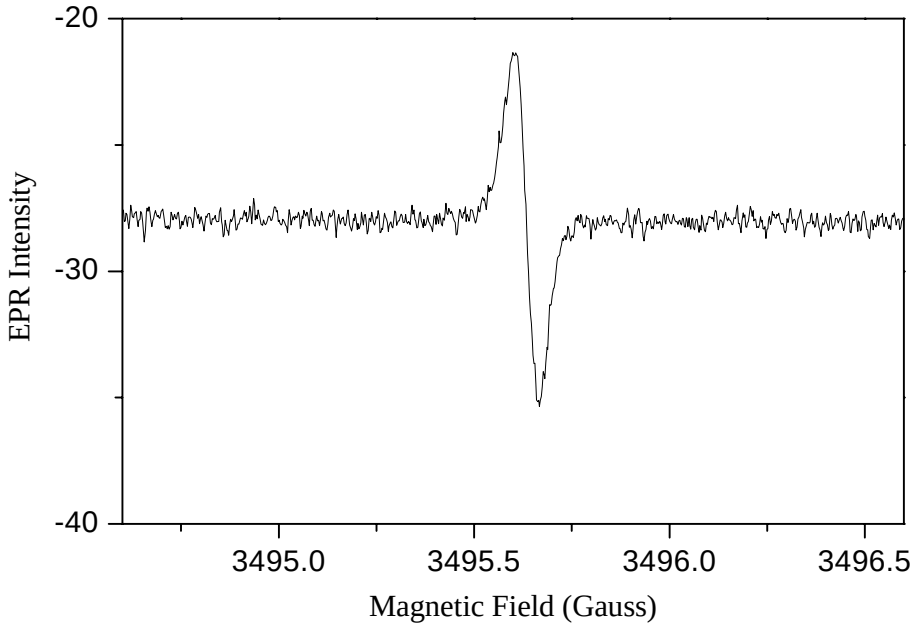

Figure 1. cw EPR spectrum of 2DEG in Si/SiGe heterostructure. The g-factor in this structure is 2.0011, essentially independent of the orientation of the magnetic field.

In Figure 1 we show a continuous wave (cw) EPR spectrum of the 2D electrons. The line is remarkably narrow, and we have seen signals as narrow as 30mG in these structures. The Si in these devices contained the natural abundance of ^{29}Si, but the electrons are free to move near many ^{29}Si atoms. The electrons average over the effective field of many magnetic nuclei as they move in the quantum well, leading to a narrow linewidth. From the measured linewidth one can estimate that the electrons occupy an area of at least about 1 μm^2.

Two experiments were performed to provide information about the spin relaxation times. In both experiments microwave pulses were used to rotate the spins about either the x or y-axes in a reference frame defined with the z-axis parallel to the static applied magnetic field, B_0, and the x- and y-axes rotating at the microwave frequency about the laboratory z-axis (A detailed explanation, including various pulse sequences, can be found in ref. 14). A 2-pulse Hahn echo experiment ($\pi/2 - \tau - \pi - \tau -$ echo) was used to measure T_2, which is directly available from the analysis of the echo decay as a function of interpulse delay, τ. The first ($\pi/2$) and second (π) pulse durations were 16 and 32 ns, respectively. A 16-step phase-cycle scheme was applied to eliminate unwanted signals, in particular the free-induction decay (FID) arising from each of the individual microwave pulses. The curve shown in Fig. 2 is an exponential fit to the data, giving $T_2 = 3.06\mu s$. The fitted curve does not pass through all the data points, especially at longer delays, indicating that there is a distribution of phase memory times.

The second experiment we performed was a 2-pulse inversion-recovery experiment ($\pi - T - \pi/2 -$ FID) which was used to measure the longitudinal relaxation time, T_1. An 8-step phase-cycle scheme was used to eliminate unwanted signals:

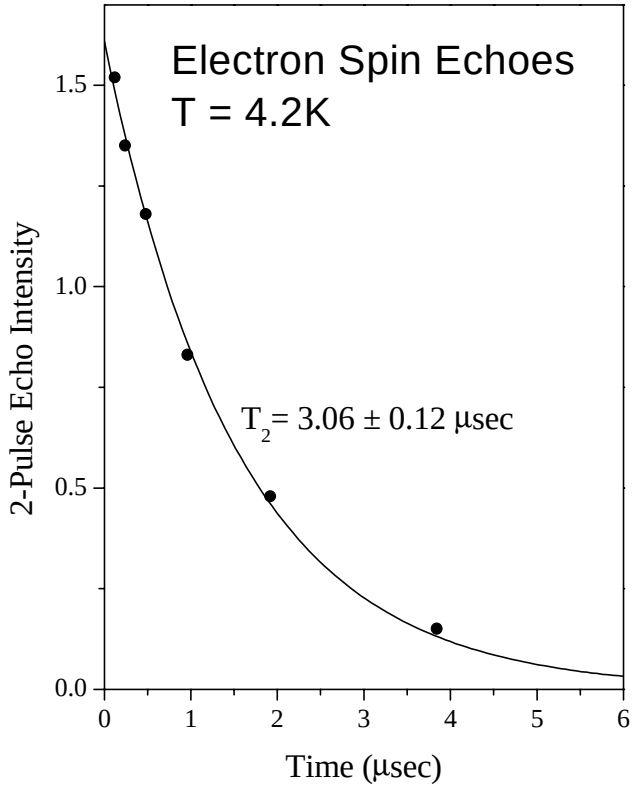

Figure 2. Echo intensity in a 2-pulse experiment ($\pi/2 - \tau - \pi - \tau -$ echo) versus total delay time (2τ). The exponential fit gives T_2. The external magnetic field, B_0, was applied perpendicular to the plane of the 2D electron system.

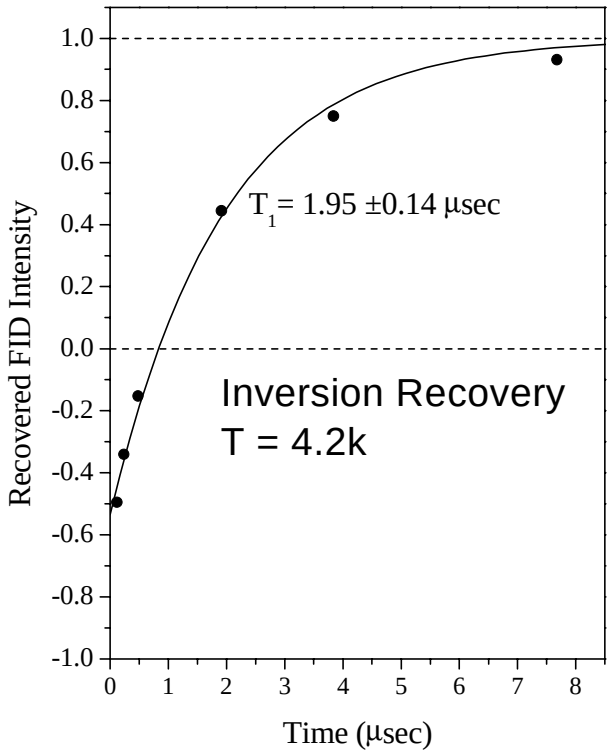

Figure 3. Recovered echo intensity in an inversion-recovery experiment ($\pi - T - \pi/2 - FID$) as a function of interpulse delay T for the 2D electron system. The exponential fit gives T_1. The external magnetic field, B_0, was applied perpendicular to the plane of the 2D electron system.

the FID from the first microwave pulse and the echo signal originating from the two pulses. The π and $\pi/2$ pulse durations were again 32 and 16 ns, respectively. For broad weak EPR lines the FID is short and lost in the cavity ring-down. To avoid this problem a third (π) microwave pulse was used to produce an echo, which is more easily detected because it is well separated in time from the applied microwave pulses. The resulting 3-pulse sequence is $\pi - T - \pi/2 - \tau - \pi - \tau -$ echo, with τ held constant at 100 ns. The results for T_1 are shown in Fig. 3. The curve in Fig. 3 is an exponential fit to the data which show $T_1 = 1.95\mu s$. As with T_2, from the quality of the fits we see that there is a distribution of longitudinal spin relaxation times.

It is particularly striking that $T_2 > T_1$ in these structures. This is an unusual situation and requires the relaxation processes to be anisotropic. From an abstract perspective, any process leading to relaxation or decoherence of a spin can be viewed as a fluctuating magnetic field acting on the spin. In the Redfield limit ($\gamma \delta B \tau_c << 1$, where γ is the electron gyromagnetic ratio, and τ_c is the correlation time of the fluctuations) and assuming that the fluctuating fields, δB, along different spatial axes are uncorrelated, the relaxation times are given by:[15]

$$\frac{1}{T_1} = \gamma^2 (\overline{\delta B_x^2} + \overline{\delta B_y^2}) \frac{\tau_c}{1 + \omega_0^2 \tau_c^2},$$

and $$\frac{1}{T_2} = \gamma^2 \overline{\delta B_z^2} \tau_c + \frac{1}{2T_1},$$

where the external magnetic field, B_0, is assumed to be applied along z direction and ω_0 is the Larmor frequency of the spin in this field. If the fluctuating fields are isotropic, T_1 is always greater than or equal to T_2. On the other hand, $T_2 = 2T_1$ if $\overline{\delta B_z^2} = 0$ and $\overline{\delta B_x^2}, \overline{\delta B_y^2} \neq 0$.

Based upon cw EPR measurements it has been suggested[16] that the spin relaxation of the 2D electrons in these Si quantum well structures is controlled by fluctuating effective magnetic fields (Rashba fields[17]) arising from the breaking of inversion symmetry by the Si/SiGe interface and the electric field in the quantum well. The Rashba fields lie entirely in the plane of the 2D electron system, resulting in $\overline{\delta B_x^2}, \overline{\delta B_y^2} > \overline{\delta B_z^2}$ which can lead to T_2 being longer than T_1. The correlation time of the field fluctuations, τ_c, should correspond approximately to the momentum relaxation time which is about 10ps for an electron in these high-mobility structures ($\mu \sim 90{,}000$ cm^2/V-sec).[18] Using this value for τ_c we estimate a fluctuating (root-mean-square) in-plane field of $\delta B_x, \delta B_y = 10$ G and the out-of-plane field fluctuations to be $\delta B_z = 5$ G to fit the measured T_1 and T_2. These field values are only estimates, since it was not possible to measure the mobility of the 2D electrons at the same time and under the same conditions as the pulsed EPR, however they are consistent with the suggestion that the Rashba effect is causing the relaxation.

While the spin relaxation times of free 2D electrons are long in comparison to some other semiconductors, times in this range are common in many materials. The situation with donor bound electrons is quite different. The longitudinal relaxation time in Si:P has already been studied in detail. At low donor concentrations ($< 10^{16}$ P/cm^3) T_1, in Si:P was found to be independent of the phosphorus concentration, and it varied from microseconds at 20 K to thousands of seconds at 2 K[19,20] The very long T_1 at low temperature is one of the main arguments for using Si as a host material. The strong temperature dependence observed in the 2-20 K range was suggested to arise from an Orbach relaxation process.[20] An energy splitting, $\Delta E = 123$ K, was derived from fast-passage experiments using cw EPR and shown to be a measure of the valley-orbit energy splitting of the P donor. Below 2 K T_1 was observed to stay approximately constant, limited by direct phonon processes.[19] The more relevant relaxation time for quantum information processing is T_2. In isotopically-purified ^{28}Si:P, $T_2 \sim 500$ μs has been previously reported,[21] while shorter times and nonexponential spin echo decays are observed in natural Si.

Four silicon samples with different phosphorus concentrations were studied: two samples with $0.8 \cdot 10^{15}$ and $1.7 \cdot 10^{16}$ P/cm^3 in natural silicon (referred to as "Si:P-10^{15}" and "Si:P-10^{16}", respectively), and two samples with $0.87 \cdot 10^{15}$ and $1.6 \cdot 10^{16}$ P/cm^3 in isotopically-purified ^{28}Si (referred to as "^{28}Si:P-10^{15}" and "^{28}Si:P-10^{16}", respectively).

The EPR spectrum of phosphorus donors in silicon consists of two lines centered at $g = 1.9992$ and split by 41.94 G due to the hyperfine interaction with the ^{31}P nucleus.[22] At 15 K and below the EPR lines have a Gaussian shape, both in Si:P and ^{28}Si:P. This indicates that an inhomogeneous line broadening is the main source of the spectral linewidth in both samples. The EPR lines in Si:P-10^{16} are much broader than those in ^{28}Si:P-10^{16} ($\Delta B = 2.5$ G and 0.08 G), reflecting the reduction in inhomogeneous broadening arising from the decreased interaction with ^{29}Si nuclei. The residual ^{29}Si concentration in the ^{28}Si:P is 800 ppm, as determined by Secondary Ion Mass Spectrometry (SIMS).[23] Most of the relaxation measurements were done on the high field component of the donor EPR spectrum, though essentially identical relaxation decays were seen at the low field component.

In the inversion-recovery experiments both the Si:P and ^{28}Si:P samples showed mono-exponential decays, and T_1 was obtained by fitting to a simple exponential. The temperature dependence of $1/T_1$ obtained for ^{28}Si:P-10^{16} at 9.7 GHz is shown with filled circles in Fig. 4. The same temperature dependence was seen for the other samples. This confirms the previous observation that T_1 is independent of P concentration (at $< 10^{16}$ P/cm^3), and also shows that T_1 does not change beyond typical run-to-run variations upon ^{29}Si-depletion.[19,21] Quite remarkably, T_1 varies by 5 orders of magnitude over the temperature interval 7-20 K. In Arrhenius coordinates, $\log(1/T_1)$ *vs.* $1/T$, the dependence is linear which is consistent with an Orbach mechanism[24] dominating the relaxation process at these temperatures ($1/T_1 \propto \exp(-\Delta E/kT)$). From the slope in this plot (dotted line) the energy gap to the excited state involved in the relaxation process is found to be $\Delta E = 126.1 \pm 0.5$ K, in good agreement with $\Delta E = 123$ K derived from the cw measurements.[20]

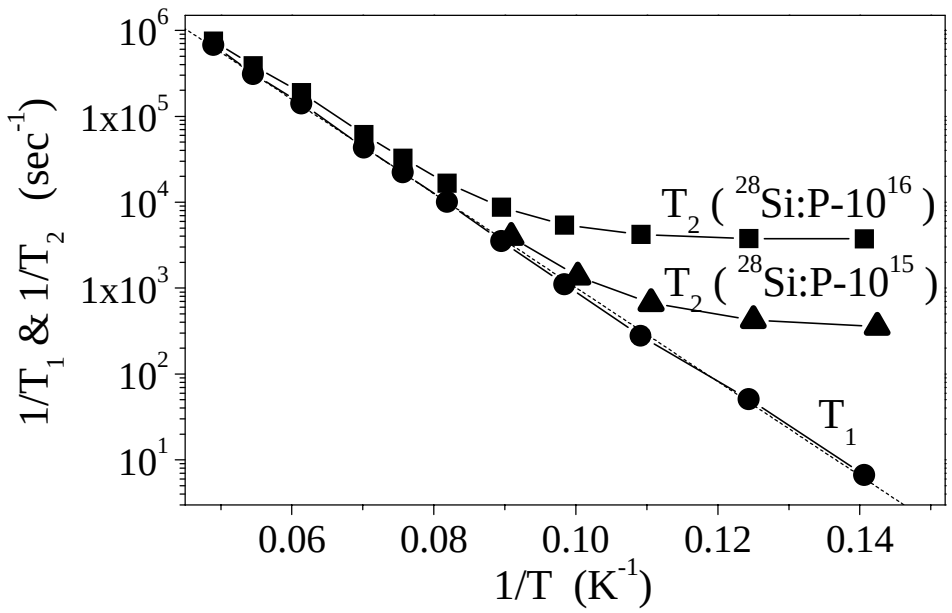

Figure 4. Temperature dependence of the longitudinal, T_1, and transverse, T_2, relaxation times in (100)-oriented Si:P. T_1 was measured with isotopically-purified ^{28}Si:P-10^{16}. T_2 is shown for two samples, ^{28}Si:P-10^{16} and ^{28}Si:P-10^{15}. All measurements shown here were made at at 9.7 GHz. The dotted line is a linear fit to the T_1 data.

From previous work it was known that T_2 saturates at considerably higher temperatures than T_1 and at considerably lower values (i.e. T_2 = 0.6 ms *vs.* $T_1 = 3 \cdot 10^3$ s at 1.2 K).[21,25] The mechanism of this saturation has not been explained. In natural Si:P non-exponential electron spin echo decays were observed, best described by $V(t) = \exp(-t/T_2 - t^3/T_S^3)$.[21,25] The cubic exponential term was explained as being caused by spin diffusion in the nuclear ^{29}Si system.[25] This suggests that in isotopically-purified ^{28}Si the term with T_S should vanish and pure exponential decays, presumably very long, should be observed. However, in their original work Gordon and Bowers reported only about a factor of 2 increase in T_2 for ^{28}Si:P over natural Si:P at 1.4 K.[21]

Figure 5 compares the 2-pulse electron spin echo (ESE) decays in isotopically-purified ^{28}Si:P-10^{15} and in natural Si:P-10^{15}. The T_2 relaxation decays in the present study were measured using a conventional 2-pulse spin echo sequence. At long inter-pulse delay, τ (> 0.3 ms), we observed significant fluctuations in the phase of the detected echo signal with respect to the phase of the microwave source. These fluctuations originate from non-ideal characteristics of the spectrometer and may result from phase instability of the microwave source or from fluctuations in the external magnetic field (B_0) during the 2-pulse experiment (these two types of fluctuation are indistinguishable in their effect on the relative phase of the echo signal). Because of this instrumental phase noise, repetitive summation of the echo signal using a conventional quadrature receiver (where the echo intensity is detected with respect to the phase of the microwave source) resulted in distorted echo decays, with a strongly non-exponential behavior (see trace labeled "quadrature detection" in Fig. 5). To avoid this instrumental problem, we implemented a different approach of signal accumulation consisting of repetitive summation of the *magnitude* of the echo signal calculated as $[(\text{in-phase})^2 + (\text{out-of-phase})^2]^{1/2}$, where "in-phase" and "out-of-phase" are the signals from the two channels of the quadrature receiver. As a result, nearly exponential decays were recovered in ^{28}Si:P over the entire range of τ (labeled "magnitude detection" in Fig. 5).

While the decay is nearly exponential in ^{28}Si:P, it is non-exponential in the natural Si:P, and well-described by $\exp(-t/T_2 - t^3/T_S^3)$. With B_0 oriented along a (100) axis of the Si crystal, T_S = 0.63 ms is estimated from the fit, and this T_S is found

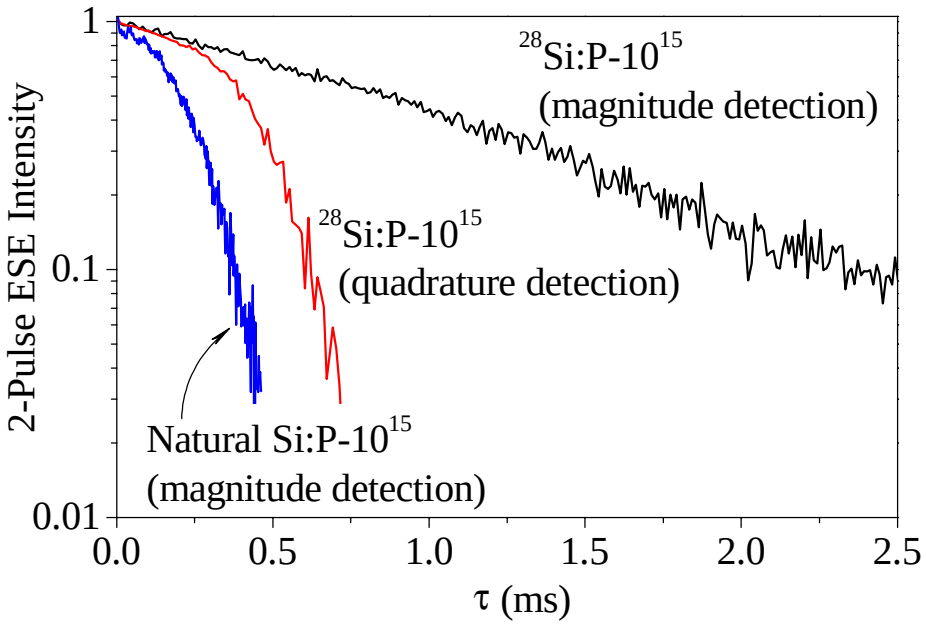

Figure 5. Semilog plot of the 2-pulse electron spin echo (ESE) decay as a function of the interpulse delay, τ for Si:P-10^{15} and ^{28}Si:P-10^{15} at 9.7 GHz. Two traces for ^{28}Si:P-10^{15} were measured as marked: by averaging of the phased echo signal (using conventional quadrature detection) and by averaging the echo magnitude (i.e. disregarding the phase of the echo signal). The faster decay seen in the "quadrature detection" approach results from non-ideal characteristics of the pulse EPR spectrometer (phase fluctuations of the microwave source and/or fluctuations of the external magnetic field).

to be temperature independent over the range 7-12 K. A shorter T_S (0.36 ms) was reported in the earlier study by Chiba and Hirai[25] but in that work the crystal was oriented differently. We found that T_S is orientation-dependent in natural Si:P, and the longest T_S is seen for a (100) orientation.

In Fig. 4 we have plotted the temperature dependence of T_2 in the two ^{29}Si-depleted samples, ^{28}Si:P-10^{16} and ^{28}Si:P-10^{15} at 9.7 GHz. Two temperature ranges are clearly seen in the T_2 data. At high temperatures, 12-20 K, T_2 follows closely and nearly coincides with T_1. Apparently, the T_1 relaxation process (the Orbach process) makes the major contribution to T_2 over this temperature range. However, at temperatures lower than 12 K for ^{28}Si:P-10^{16} and lower than 10 K for ^{28}Si:P-10^{15}, T_2 diverges from T_1. While T_1 continues to grow, approaching to $3\cdot10^3$ s at 1.2 K,[19] T_2 becomes temperature-independent and saturates at 0.27 and 2.8 ms in ^{28}Si:P-10^{16} and ^{28}Si:P-10^{15}, respectively. The fact that the limiting value of T_2 is greater in the sample with smaller P concentration suggests that T_2 at low temperatures is mostly determined by the dipole-dipole interaction between neighboring P-donors via instantaneous diffusion.[26] This effect is known to be temperature-independent, given that the T_1 of the spins involved is long compared to the total duration of the 2-pulse experiment.[27]

To test this hypothesis, 2-pulse echo experiments ($\pi/2 - \tau - \theta_2 - \tau$ – echo) with a variable rotation angle, θ_2 of the second microwave pulse were performed. The results obtained at 6.9 and 8.1 K are plotted in Fig. 6. It is seen that $1/T_2$ varies linearly with $\sin^2(\theta_2/2)$ indicating that, indeed, instantaneous diffusion contributes significantly to the observed T_2 relaxation rates at these temperatures. Linear fits were obtained assuming the same slope for both data sets, and the resulting slope was $(3.2 \pm 0.2)\cdot10^2$ s^{-1}, which is close to $3.5\cdot10^2$ s^{-1} as expected for a homogeneous P-distribution[28] at $0.87\cdot10^{15}$ P/cm^3. Extrapolation to $\theta_2 = 0$ (to eliminate the contribution of instantaneous diffusion) gives $1/T_2 = 0.072 \pm 0.008$ and 0.016 ± 0.007 ms^{-1} at 8.1 K and 6.9 K, respectively. The corresponding intrinsic T_2 values (of the isolated

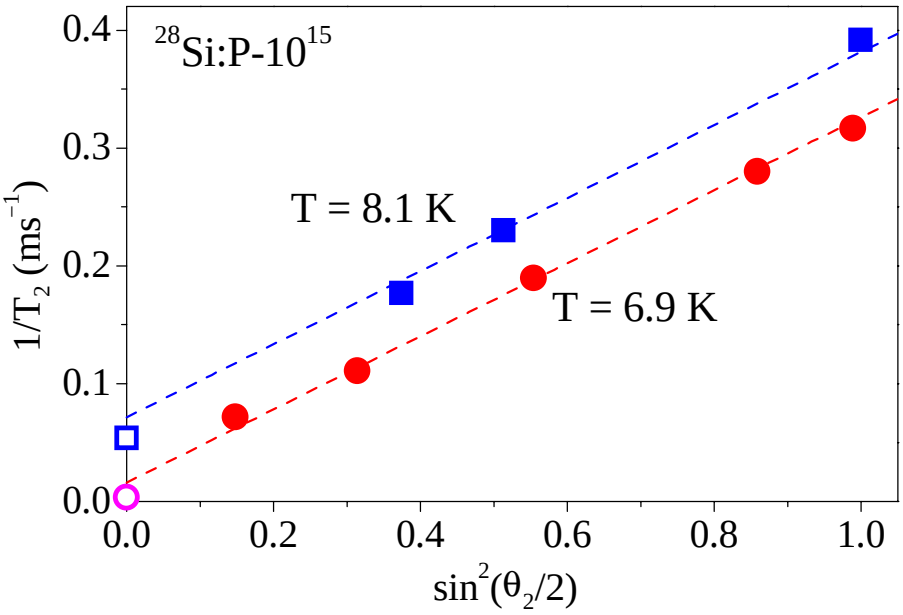

Figure 6. Demonstration of the instantaneous diffusion contribution to T_2 in ^{28}Si:P-10^{15}, at 9.7 GHz and temperatures 8.1 and 6.9 K. $1/T_2$ (solid symbols) is plotted as a function of the turning angle (θ_2) of the second microwave pulse in a 2-pulse spin echo experiment. Open symbols on the y-axis indicate $1/T_1$ at the respective temperatures. The slope of the linear fit (dashed lines) is proportional to the P concentration and the intercept corresponds to the intrinsic T_2 of an isolated donor-electron spin at that temperature.

donor-electron spins in ^{28}Si:P) are 14 ± 2 ms at 8.1 K and 62 (+50/-20) ms at 6.9 K and approach the T_1 values at these temperatures (18.5 and 280 ms, respectively).

From the experimental data shown here, it is clear that exceptionally long qubit coherence times can be seen if the qubits are the spin of electrons, the electrons are tightly bound in a Si host, and the ^{29}Si is removed. Here we have used donors to bind the electrons, but artificial quantum dots should work nearly as well. One expects that the decoherence will be governed by an Orbach process, with the activation energy being the energy to the first excited state. If the quantum dot is formed at a heterointerface, as is the usual case, the prefactor in the exponential dependence will be larger than for the donor since the spin-orbit coupling is enhanced by the loss of inversion symmetry. However, lower temperatures will be necessary for quantum information processing, in any case, to freeze the spins into their ground state with high efficiency.

In addition to decoherence, the spin-orbit interaction at the interface will introduce other complications into the reliable operation of a quantum information processor. By coupling the spatial part of the electrons' wavefunctions to their spin components, the splitting between spin-up and spin-down becomes a function of their spatial state. This is nothing more than the statement that the g-factor of the electrons bound in quantum dots will be a function of the details of their wavefunctions. Slight differences in the dot shapes will cause the electron spins to precess at slightly different rates in a magnetic field. However, these differences can probably be cancelled by periodic refocusing (π) pulses of microwaves. In most proposals for spin-based quantum computing in semiconductors the spin-spin interactions required to entangle spins are produced by controlling the exchange interaction between nearby electrons.[1-4] Turning on and off the exchange interaction between electrons in adjacent quantum dots requires distorting their wavefunctions to force them to

overlap for a short time. This distortion will cause a precession of the spins through the spin-orbit coupling, but under certain circumstances it can be shown that well-behaved quantum gates are still feasible.[29]

The spin-orbit interaction arising at a heterointerface does not make quantum information processing by spins in semiconductors impossible, but it does significantly raise the level of difficulty. The fact that the coherence time is reduced for unbound electrons makes the movement of electrons over large distance problematical. Low-coherence transport requires that quantum information must be propagated through a series of swap operations rather than by simply transporting the electron. There are several straightforward approaches to lengthening the coherence time of the 2D electrons. The Si quantum wells used in the experiments discussed above were one-side modulation doped. This produces the maximum asymmetry and thus the maximum Rashba field. More symmetric wells and doping should reduce the Rashba field by probably as much as an order of magnitude. Also, at the B_0 used in these experiments $\omega_0\tau_c$ is approximately one, which leads to a maximum decoherence rate. By operating at higher magnetic fields the spin precession frequency will be higher and T_2 will be further lengthened.

A rather different approach to reducing the effect of the spin-orbit coupling is to change the host material. Carbon is lighter than Si, and shows smaller spin-orbit effects. The only stable isotope of carbon with a nuclear magnetic moment is ^{13}C, and it occurs naturally with a concentration of 1%. Isotopically purified ^{14}C is readily available. However, the technology for moving and manipulating electrons is less well-developed for crystalline C (diamond) than for Si. However, entirely different approaches to quantum information processing have been proposed based upon carbon nanotubes and fullerenes.[30]

If the host material can be completely eliminated, the spin-orbit effects can be reduced even further. This can be accomplished by floating the electrons on the surface of superfluid helium.[31] The electrons are bound to the helium by their image charge,[32] and to a first approximation the system can be thought of as the equivalent of a semiconductor heterointerface with the interface being between the liquid helium and the vacuum. Electrons can be controlled by gates in a similar fashion as they are in a semiconductor, but with the added constraint that the interface is required to be oriented with respect to the gravitational field.[33] The electron is in a vacuum, and thus the atomic part of the spin-orbit interaction is eliminated. There will still be a magnetic field arising from the electron moving across the helium surface while being held there by a perpendicular electric field. Using conservative values of for the electron velocity on the helium surface (10^6cm/sec) and the perpendicular electric field (10^4 V/cm), one finds obtains a "spin-orbit field" of about 1mG. This is to be compared to the 10 G Rashba field we found for electrons at a Si/SiGe interface. As discussed above, this field enters the decoherence as the square, giving coherence times of hours without the need to localize the electrons. Thus certain aspects of spin-based quantum computing are intrinsically simpler with electrons floating on liquid helium than in a semiconductor.

In summary we have measured the spin coherence times for both free and bound electrons in Si. In isotopically enriched Si, with few magnetic nuclei, the spin coherence time is exceptionally long. The T_2 of an isolated donor electron spin is at least 60ms, and is probably longer. We are currently instrument-limited in measuring longer times. For free electrons at a Si/SiGe heterointerface, we measure a T_2 of about 3 μsec. This time appears to be determined by the spin-orbit coupling in the form of the Rashba effect. Confining the electrons to artificial quantum dots at an interface should lengthen T_2, as for the donors, but this spin-orbit interaction adds a number of complications to the operation of quantum gates. Systems with smaller spin-orbit couplings are thus interesting to consider. Amongst the semiconductors, carbon either as diamond or as nanotubes and fullerenes should exhibit smaller spin-orbit complications. However, it also appears very promising to go to the limit of holding the electron in a vacuum, floating on the surface of liquid helium. This configuration minimizes the spin-orbit effects, and decoherence rates are about 8 orders of magnitude lower than we have measured in Si 2DEG structures.

The author would like to thank A. Tyryshkin, W. Jantsch, F. Schäffler, A. Raitsimring, and A. Astashkin for collaborations on this work. He would also like to thank the ARO and ARDA under Contract No. DAAD19-02-1-0040, the DARPA's SPINS Program through Los Alamos National Lab, and the NSF through the International Office and the MRSEC program.

REFERENCES

1. D. Loss and D.P. DiVincenzo, "Quantum Computation with Quantum Dots," *Phys. Rev. A* **57**, 120 (1998).
2. B.E. Kane, "A Silicon – Based Nuclear Spin Quantum Computer," *Nature* **393**, 133 (1998).
3. R. Vrijen, E. Yablonovitch, K. Wang, H.W. Jiang, A. Balandin, V. Roychowdhury, T. Mor, and D. DiVincenzo, "Electron-Spin Resonance Transistors for Quantum Computing in Silicon – Germanium Heterostructures," *Phys. Rev. A* **62**, 012306 (2000).
4. Mark Friesen, Paul Rugheimer, Donald E. Savage, Max G. Lagally, Daniel W. van der Weide, Robert Joynt, and Mark A. Eriksson, "Practical design and simulation of silicon-based quantum-dot qubits," *Phys. Rev. B* **67**, 121301 (2003).
5. C. P. Slichter, *Principles of Magnetic Resonance, 2nd edn*, (Springer, Berlin, 1980).
6. R. W. Equall, Y. Sun, R. L. Cone, and R. M. Macfarlane, "Ultraslow optical dephasing in Eu^{3+}:$Y_2SiO_{5,}$" *Phys. Rev. Lett*. **72**, 2179 (1994).
7. G. Dresselhaus, "Spin-Orbit Coupling Effects in Zinc Blende Structures," *Phys. Rev*. **100**, 580 (1955).
8. L. Liu, "Valence Spin-Orbit Splitting and Conduction g Tensor in Si," *Phys. Rev. Lett*. **6**, 683 (1961).
9. A. M. Tyryshkin, S. A. Lyon, A. V. Astashkin, and A. M. Raitsimring, "Electron spin relaxation times of phosphorus donors in silicon," *Phys. Rev. B* **68**, 193207 (2003).
10. A.M. Tyryshkin, S.A. Lyon, W. Jantsch, F. Schäffler, "Spin Manipulation of Free 2-Dimensional Electrons in Si/SiGe Quantum Wells," e-print cond-mat/0304284.
11. C.F.O. Graeff, M.S. Brandt, M. Stutzmann, M. Holzmann, G. Abstreiter, and F. Schäffler, "Electrically detected magnetic resonance of two-dimensional electron gases in Si/SiGe heterostructuresv," *Phys. Rev. B* **59**, 13242 (1999).
12. W. Jantsch, Z. Wilamowski, N. Sandersfeld, and F. Schäffler, "ESR Investigations of Modulation-Doped Si/SiGe Quantum Wells," *Phys. Stat. Sol. B* **210**, 643 (1998).
13. Z. Wilamowski, N. Sandersfeld, W. Jantsch, D. Többen, and F. Schäffler, "Screening Breakdown on the Route toward the Metal-Insulator Transition in Modulation Doped Si_SiGe Quantum Wells," *Phys. Rev. Lett*. **87**, 026401 (2001).
14. A. Schweiger and G. Jeschke, *Principles of Pulse Electron Paramagnetic Resonance*, (Oxford University Press, Oxford, 2001).
15. Y. Yafet, *Solid State Physics*, **14**, 1 (Academic Press, New York, 1963).
16. Z. Wilamowski, W. Jantsch, H. Malissa, and U. Rössler, "Evidence and evaluation of the Bychkov-Rashba effect in SiGe/Si/SiGe quantum wells," *Phys. Rev. B* **66**, 195315 (2002).
17. Yu. A. Bychkov and E.I. Rashba, "Oscillatory effects and the magnetic susceptibility of carriers in inversion layers," *J. Phys. C* **17**, 6039, (1984).
18. D. Tobben, F. Schaffler, A. Zrenner and G. Abstreiter, "Magnetotransport measurements and low-temperature scattering times of electron gases in high-quality $Si/Si_{1-x}Ge_x$ heterostructures," *Phys. Rev. B* **46**, 4344 (1992).
19. G. Feher and E.A. Gere, "Electron Spin Resonance Experiments on Donors in Silicon. II. Electron Spin Relaxation Effects," *Phys. Rev*. **114**, 1245 (1959).
20. T.G. Castner, "Direct Measurement of the Valley-Orbit Splitting of Shallow Donors in Silicon," *Phys. Rev. Lett*. **8**, 13 (1962).
21. J. P. Gordon and K. D. Bowers, "Microwave Spin Echoes from Donor Electrons in Silicon," *Phys. Rev. Lett*. **1**, 368 (1958).
22. G. Feher, "Electron Spin Resonance Experiments on Donors in Silicon. I. Electronic Structure of Donors by the Electron Nuclear Double Resonance Technique," *Phys. Rev*. **114**, 1219 (1959).
23. K. Itoh, private communication.
24. R. Orbach, "Spin-Lattice Relaxation in Rare-Earth Salts," *Proc. Phys. Soc*. (Lond.) **77**, 821 (1961).
25. Meiro Chiba and Akira Hirai, *J. Phys. Soc Jap*. **33**, 730 (1972).
26. J. R. Klauder and P. W. Anderson, "Spectral Diffusion Decay in Spin Resonance Experiments," *Phys. Rev*. **125**, 912 (1962); W. B. Mims, "Phase Memory in Electron Spin Echoes, Lattice Relaxation Effects in $CaWO_4$:Er, Ce, Mn ," *Phys. Rev*. **168**, 370 (1968).
27. K. M. Salikhov, et al., *J. Magn. Reson*. **42**, 255 (1981).
28. A. M. Raitsimring, et al., *Sov. Phys. Solid State* **16**, 492 (1974).
29. D. Stepanenko, N. E. Bonesteel, D. P. DiVincenzo, G. Burkard, and D. Loss, "Spin-orbit coupling and time-reversal symmetry in quantum gates," *Phys. Rev. B* **68**, 115306 (2003).
30. W. Harneit, "Fullerene-based electron-spin quantum computer," *Phys. Rev. A* **65**, 032322 (2002).
31. S.A. Lyon "Spin-Based Quantum Computing Using Electrons on Liquid Helium," e-print cond-mat/0301581.
32. C.C. Grimes, "Electrons in Surface States on Liquid Helium," *Surf. Sci*. **73**, 379 (1978) and references therein.
33. P. Glasson, S. Erfurt Andresen, G. Ensell, V. Dotsenko, W. Bailey, P. Fozooni, A. Kristensen, and M.J. Lea, "Microelectronics on liquid helium," *Physica B* **284-288**, 1916 (2000).